Article ID: 1006-8775(2010) 03-0292-07

# HIGH-RESOLUTION NUMERICAL SIMULATION OF WIND ENERGY RESOURCE IN HAINAN PROVINCE AND ITS OFFSHORE WATERS

XING Xu-huang (邢旭煌)[1,2], ZHU Rong (朱　蓉)[3], ZHAI Pan-mao (翟盘茂)[4], YU Wei (俞　卫)[5]

(1. College of Atmospheric Sciences, Lanzhou University ,Lanzhou 730000 China; 2. Hainan Climate Center, Haikou 570203 China; 3. National Climate Center, Beijing 100081 China; 4. China Meteorological Administration, Beijing 100081 China; 5. Meteorological Research Branch, Environment Canada, Quebec)

**Abstract:** With high resolution (1 km), the distribution of wind energy resources in Hainan province and over its offshore waters is numerically simulated by using the Wind Energy Simulation Toolkit (WEST) model developed by Meteorological Research Branch of Environment Canada. Compared with observations from eight coastal anemometric towers and 18 existing stations in the province, the simulations show good reproduction of the real distribution of wind resources in Hainan and over its offshore waters, with the relative error of annual mean wind speed being no more than 9% at the 70-m level. Moreover, based on the simulated results of WEST grids that are closest to where the eight wind towers are located, the annual mean wind speeds are further estimated by using the Danish software WasP (Wind Atlas Analysis and Application Program). The estimated results are then compared with the observations from the towers. It shows that the relative error is also less than 9%. Therefore, WEST and WEST+WAsP will be useful tools for the assessment of wind energy resources in high resolution and selection of wind farm sites in Hainan province and over its offshore waters.

**Key words:** wind energy resources; Wind Energy Simulation Toolkit (WEST); wind speed; high resolution; numerical simulation

**CLC number:** P425.6.3 **Document code:** A **doi:** 10.3969/j.issn.1006-8775.2010.03.011

## 1 INTRODUCTION

Because of regular resources shortage and environment pollution, the whole world is now seeking to exploit reproducible and clean energy resources. With the advantage of mature wind power generation technology and capability of large-scale commercial exploitation, wind energy is developing with the highest speed among all the reproducible clean energy resources. At the present time, wind power generation is mainly developed in onshore areas. With the continuous decrease of available land, however, many countries have shifted the wind power generation to offshore waters. It is of great development potential to exploit wind energy resources over offshore waters because of the merits of low surface roughness, mild turbulence, abundant wind energy resource and tremendously available areas.

Much research has been done by institutions and individuals in China and abroad on harnessing offshore wind energy. The 1993 project, "Study of Offshore Wind Energy in the EC," sponsored by European Union Committee, assessed the offshore wind energy in 12 European countries. Walmsley et al.[1] analyzed offshore wind energy using statistics based on coastal meteorological data. Lange et al.[2] found a correlationship using data observed synchronously from overland and offshore stations, and evaluated offshore energy by extrapolating the long-term coastal observations with Wind Atlas Analysis and Application Program (WAsP). Yuan et al.[3] conducted simulation analysis of offshore wind fields by using a mesoscale meteorological model MM5. Jiang et al.[4] researched the assessment of offshore wind energy by space information technologies.

An early study on offshore wind energy in China used extrapolation based on observations of overland meteorological stations. In the last decade, a new round of offshore wind energy assessment has been initiated

**Received date:** 2009-12-10; **revised date:** 2010-06-01

**Foundation item:** Project for Popularization of Advanced Meteorological Technology for 2006, China Meteorological Administration (CMATG2006M41)

**Biography:** XING Xu-huang, B.S., senior engineer, primarily undertaking research on climate change and exploration/utilization of climatic resources.

E-mail for corresponding author: xingxuhuang@sina.com.cn

in coastal provinces, comprising mainly statistical analysis of historical observations from coastal meteorological stations, oceanic stations, and island stations, together with some data observed by short-term island towers. These works, however, cannot satisfy the need to fully harness offshore wind energy. A number of technologies are being used to study offshore wind energy. Mesoscale and microscale numerical simulation models are being developed rapidly in the study of wind energy exploitation to deal with the limitations of data distribution and length of observational time. Although numerical simulation cannot take the place of onsite observation, simulating lower atmospheric wind field can make up the shortage of observations in order to reduce the uncertainties of wind energy assessment to a certain extent and speed up the site selection of wind power station. The lack of existing wind energy study techniques has the China Meteorological Administration (CMA) imported the Canadian software Wind Energy Simulation Toolkit (WEST), and CMA has promoted it with Meteorological Research Branch of Environment Canada to provide technical support in the study of wind energy distribution.

## 2 INTRODUCTION TO MODEL

### 2.1 *Experiment design*

Based on the theory of statistics and dynamics of downscaling[5], WEST was developed by Environment Canada for the exploration of wind energy. WEST is used to assess the wind energy resource. As it is impossible to conduct long-term numerical simulations of climate because of limited duration of validation, it is common to combine the methods of statistics and dynamics.

Surface wind is formed by the geostrophic wind in the near-surface layer and the friction of the underlying surface. First, with the assumption that the geostrophic wind is homogenous in a limited area, WEST classifies the geostrophic wind into different types according to the speed, direction, and vertical shear of the wind. These data are used as the initial values of the large-scale weather background field in a mesoscale model. Then, the underlying surface with steady terrain and the roughness are used as the boundary conditions to drive the mesoscale model to simulate wind conditions with high resolution in different weather background fields. Finally, the frequencies for these background fields that appear in the whole climate zone are weight-averaged to determine the distribution of wind energy resources. Refer to Fig. 1 for detailed procedure flow.

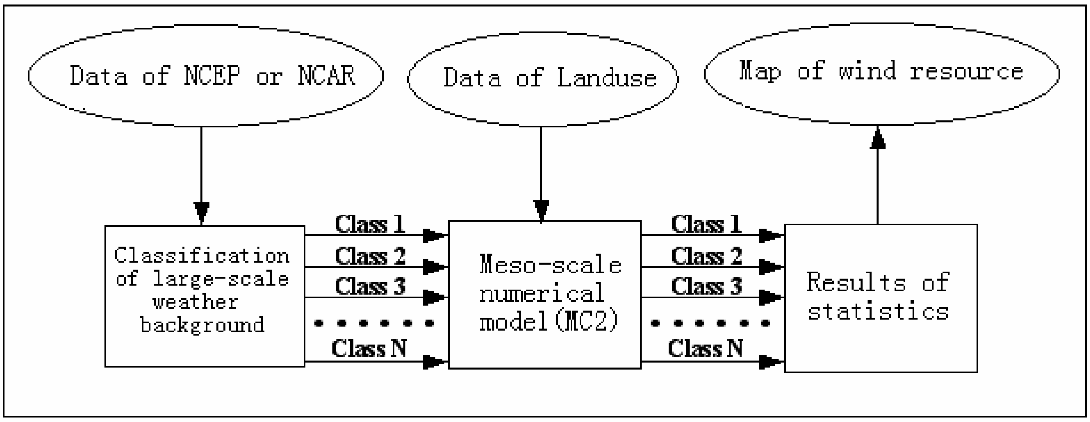


Fig. 1. Flowchart of WEST model

The geostrophic wind in the surface layer of WEST is determined through calculation of the U.S. National Centers for Environmental Prediction (NCEP) reanalysis of pressure, temperature, and humidity with a resolution of 2.5°×2.5° for the four levels (1 000, 850, 700, and 500 hPa) that are available four times a day. Upon categorization of geostrophic wind according to speed, direction, and vertical shear, wind speed was divided into 14 scales of unequal intervals; wind direction was divided into 16 directions of equiangular distance; and vertical shear was divided into positive and negative values between the levels of 1 000 hPa and 850 hPa. The vertical shear was not taken into account in the lowest scale of wind speed; therefore, there were 14×16×2-16=432 kinds of wind speed at most. Generally, when WEST is used to simulate the wind condition in a certain area, the amount of calculation is so massive that the study area has to be divided into different boxes. The number of boxes is decided by the size of the area, the resolution of the simulation, and the condition of computation. Since the geostrophic wind is assumed to be homogenous as the initial field for the mesoscale model, when simulation is performed with WEST, the weather background fields need to be characterized in only a number of grid points in a limited area.

The mesoscale model of WEST is referred to as the mesoscale compressible community model (MC2)[6-8]. This model is based on the following: a compressible hydrostatic approximate equilibrium, semi-Lagrangian scheme, semi-implicit finite difference scheme, and terrain-following coordinate system. It can be used in numerical weather prediction with high resolution (1–5 km). Based on the vertical profile relation between the near-surface wind speed and temperature, as indicated in the statistical module, the condition of wind at any height can be determined through interpolation and weighted averaging, such as average wind speed, wind power intensity, and others.

In addition, WEST can output two data sets: a wind direction frequency data set in 12 equiangular sectors (centered at 0°, 30°, 60°…330°) and an occurrence data set for wind speed of different scale in these equiangular sectors. These two data sets can be input into a microscale model (WAsP) in order to simulate wind energy resource at a higher resolution.

### 2.2 *WAsP software*

WAsP was developed by Risoe National Laboratory in Denmark for the layout and design of a wind field. WAsP can be applied to the evaluation of wind energy, the arrangement of wind turbines, the estimation of electricity output, and so on.

The principle of WAsP is as follows[9]. First, suppose the geostrophic wind in a certain area is steady and the surface wind is formed under the friction of geostrophic wind and the ground. The relationship between them is, at some point, equilibrious. The variation of the wind in the surface layer at different height can be described by the following equation: $U(z)=\frac{u_*}{k}\ln(z/z_0)$. If the condition of the wind in a certain place and at a certain time and the surface roughness length $Z_0$ are known, the geostrophic wind in an ideal condition for that area can be computed. Therefore, if the roughness length of a certain place is known, the condition of the wind for that place can be calculated. As the probability distribution generally meets the Weibull distribution, the intensity of wind power can be calculated. If the power curve of a wind turbine is known, the amount of electricity output can be computed.

WAsP comprises four main modules: analysis of raw wind measurements, generation of wind atlas, assessment of wind condition, and theoretical calculation of electricity output.

## 3 DATA AND METHODS USED IN THE ANALYSIS

### 3.1 *NCEP/NCAR data*

U.S. NCEP/National Center for Atmospheric Research (NCAR) reanalysis is a global assimilation data set obtained after applying quality control and assimilation to observations from the ground, ships, radiosonde, pilot balloons, airplanes, and satellites by its assimilation processing system of global climate data[10]. This data set includes three categories: isobaric surfaces (at 17 levels), ground surface, and flux, totaling 32 fields of elements. Each field is distributed globally with a resolution of 2.5°×2.5° or T62 Gaussian grid points (192×94 grid points). In the research of variation of climate, NCEP/NCAR reanalysis is analyzed and studied as diagnostic data[11-13]. In the simulation and prediction of global and regional climate change, NCEP data are used as the initial field and driving field for climate models[14-15].

### 3.2 *Data of terrain and ground surface*

The data of global terrain and ground surface with different resolution in WEST, obtained from categorized information of satellites, are from the U.S. Geological Survey (USGS). The characteristic quantities of ground surface in WEST mainly include Land Sea Mask, Topography [DEM], Vegetation Index, Sand, Clay, Urban Type, and others. In the WEST model, the characteristic values of surface can be modified manually or using programs in order to reflect the latest surface condition for a given area.

### 3.3 *Data of meteorological stations*

The wind measurements (height of 10 m) in 18 meteorological stations in Hainan province span from 1971 to 2000. The data of annual average wind speed are the average at four fixed times: 0200, 0800, 1400, and 2000 (Beijing Standard Time, or BST, same below).

### 3.4 *Data of wind towers*

There were eight 70-m tall anemometer towers near the northern and western coast (Fig. 2). The ground around these towers was relatively flat, and the obstacles around the towers were relatively low. At every level of each tower (10, 30, 50, and 70 m), there was a type of shaft running anemometer (SecondWind, U.S.A.). The cup anemometers on all the towers were standardized by the equipment-testing department of China Meteorological Administration. The equipment sampled data every 1 s; output of data was once every 10 min. In this paper, the data obtained from these towers span from September 2005 to August 2006; the annual average wind speed is based on the mean for all values of hourly wind speed.

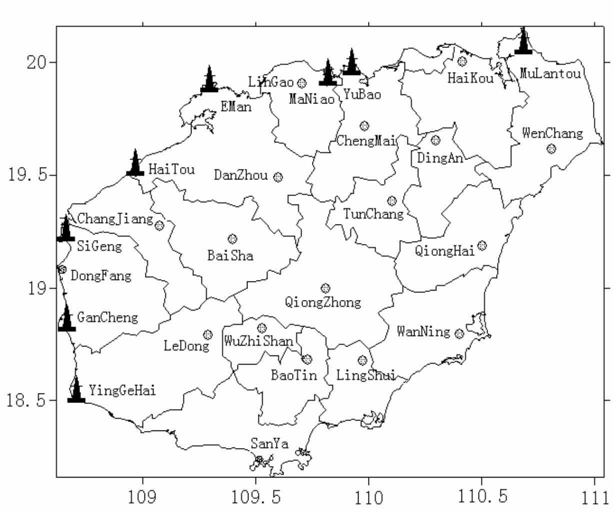


Fig. 2. Location of anemometer towers and meteorological stations in Hainan province

## 4 COMPARISON OF MEASURED AND SIMULATED VALUES WITH WEST MODEL

### 4.1 *Simulation scheme*

In order to compare the measured values between stations and anemometer towers smoothly and test the performance of the model, two simulations were carried out. The resolution of the simulations was 1 km, and the regional range was 17.61°N–20.57°N, 107.98°E–111.74°E.

The simulation was conducted as follows. First, the large-scale weather background field is classified based on the NCEP reanalyzed data in certain timeframes (30 years or 1 year) to determine the data of the background field in the simulated area. Second, data of terrain and roughness length of the surface in the simulated area are obtained with the same resolution as in the mesoscale model. Third, mesoscale simulation is conducted. Fourth, statistics of the annual average wind speed and intensity of wind power are obtained at random heights, such as 10 or 50 m or any other height, in the simulated area.

### 4.2 *Numerical simulations and effect tests of wind energy resources for the 30 years*

To test the effect of the simulation of the model, a comparison between the simulated and measured values is necessary. The simulated value for a given point is the weighted average based on the distance of the simulated value in four surrounding grid points. In this way, the average wind condition can be reflected for the point in a given range. There only exists anemometric data for the height of 10 m at the meteorological stations; therefore, the average simulated values of wind speed were extracted at the corresponding height (10 m) of the 18 meteorological stations for the past 30 years to compare with the measured values of the stations (Fig. 3). Results show that the simulated values were larger than the measured ones; for some stations, the difference was much larger. However, the correlation coefficient is high between these two kinds of value, being 0.826, and passes significance tests with a significance level of 0.01, showing consistent spatial distribution between the simulated and measured values. The average simulated value of wind speed was analyzed for the heights of 10, 30 and 50 m in Hainan province (Fig. 4). The average wind speed was larger at sea west and south off the island and along the coast than that in the central region (except for a limited area of a mountain range). The spatial distribution of the average simulated wind speed tends to be consistent with that of the average wind speed measured at the height of 10 m in a general survey of wind energy (the third one of its kind) in Hainan province.

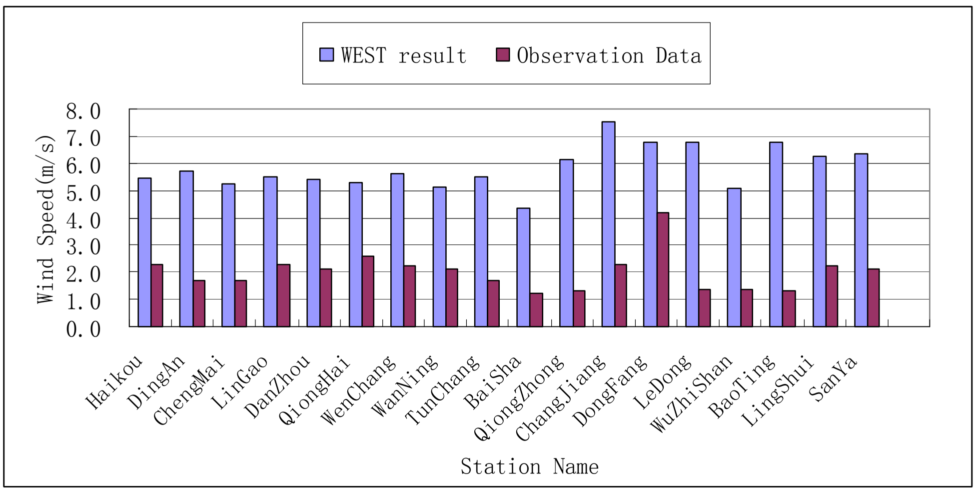


Fig. 3. Comparison between the simulated value with WEST model and measured value at the height of 10 m in Hainan province

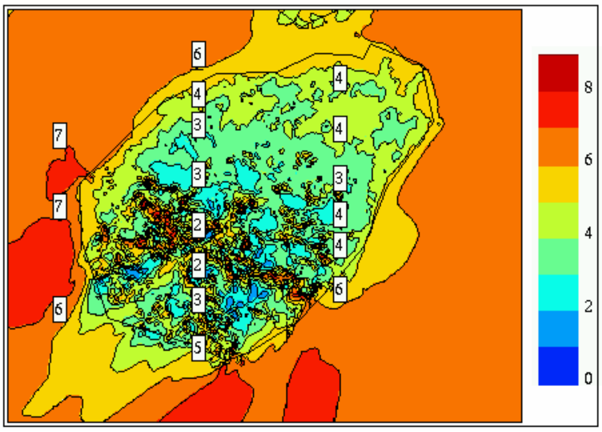

Fig. 4. Average WEST simulated values of wind speed at 50 m for 30 years in Hainan province (Unit: m/s)

### 4.3 *Numerical simulation and effect test of wind energy resource for one year*

In order to compare smoothly with the one-year data collected at the four levels of the anemometric towers and make corresponding one-year numerical simulation, the statistics of the annual average wind condition were determined at the four heights (10, 30, 50 and 70 m). The location of the eight anemometric towers enabled them to represent the climate over adjacent areas. As a result, the average simulated values of wind speed collected at the corresponding heights of the eight towers were directly compared with the measured values collected from the towers (Table 1). The table shows that, except for the absolute errors between the simulated values and measured values in Haitou and Mulantou at the height of 10 m (1.2 and 1.0 m/s, respectively), other absolute errors are less than 1.0 m/s. Specifically, the absolute error in Sigeng, which is near the coastline and with flat terrain, differs by merely 0.1–0.3 m/s. In addition, the absolute error variation corresponds to the change in height. The higher a point is located, the smaller the absolute error. Haitou is an example of a low-level point with large absolute errors: at the height of 10 m, the absolute error is 1.2 m/s, while at the height of 70 m, it is 0.0 m/s. The variation is attributed to the surrounding environment. The anemometric tower in Haitou is distant from the coast (approximately 1.5 km), and the land is covered with many hillocks and coconut palms of several meters in height. The anemometric tower is just located in a valley between the hillocks, probably accounting for the relatively large absolute error between average simulated values and measured values of wind speed in Haitou. In general, the effect of WEST is better for the western coastal regions of Hainan province and more elevated locations (such as 70 m). This height is appropriate for the wind turbines built with present technologies.

Table 1. Comparison between WEST-simulated values and measured values from the eight anemometric towers in terms of average wind speed at different height

| Tower Name | 10 m | | | 30 m | | |
|---|---|---|---|---|---|---|
| | WEST (m/s) | Tower/ (m/s) | Relative err. / % | WEST (m/s) | Tower/ (m/s) | Relative err. / % |
| Yinggehai | 3.5 | 3.7 | 4 | 4.1 | 4.8 | 15 |
| Gancheng | 5.8 | 5.2 | 12 | 6.5 | 6.4 | 1 |
| Sigeng | 5.1 | 5.2 | 2 | 5.9 | 5.8 | 1 |
| Haitou | 4.7 | 3.5 | 35 | 5.2 | 4.5 | 16 |
| Emang | 5.0 | 4.4 | 15 | 5.7 | 5.5 | 3 |
| Maniao | 4.8 | 4.6 | 5 | 5.4 | 5.8 | 8 |
| Yubao | 4.4 | 4.2 | 4 | 5.1 | 5.6 | 9 |
| Mutoulan | 5.4 | 4.4 | 22 | 6.1 | 6.5 | 7 |
| Tower Name | 50 m | | | 70 m | | |
| | WEST (m/s) | Tower/ (m/s) | Relative err. / % | WEST (m/s) | Tower/ (m/s) | Relative err. / % |
| Yinggehai | 4.3 | 5.0 | 14 | 4.7 | 5.1 | 9 |
| Gancheng | 6.8 | 6.7 | 2 | 7.0 | 6.8 | 3 |
| Sigeng | 6.2 | 6.5 | 4 | 6.5 | 6.7 | 2 |
| Haitou | 5.5 | 5.0 | 9 | 5.7 | 5.7 | 0 |
| Emang | 5.9 | 6.2 | 5 | 6.1 | 6.6 | 8 |
| Maniao | 5.6 | 6.1 | 8 | 6.1 | 6.5 | 6 |
| Yubao | 5.6 | 6.0 | 10 | 6.0 | 6.4 | 7 |
| Mutoulan | 6.4 | 7.0 | 9 | 6.7 | 7.2 | 7 |

## 5 EFFECT TEST FOR WASP ASSESSMENT OF WIND CONDITION SIMULATION

To test the effect of WAsP on the assessment of wind condition in a certain area, the Yubao and Maniao towers were chosen because of their closeness to each other (7 km apart). Based on the measured wind speed in the Yubao anemometric tower at the four different heights (10, 30, 50 and 70 m), the average wind speeds were estimated for the nearby Maniao anemometric tower by WAsP; 16 estimated values were determined. These values were compared with the measured values of the Maniao tower. According to Table 2, the estimated values of the Maniao tower at the four different heights by WAsP have little difference from the measured values. These values are almost the identical when the height of Yubao for actual measurements is the same as the height of Maniao for estimation. This may be attributed to the short distance between the two towers and the flat terrain nearby. Therefore, it follows that the WAsP-based assessment of wind condition for the region could be reliable.

Table 2. Comparison between estimated value (horizontal) by WAsP based on the measured value of Yubao and the measured value of average wind speed in the Maniao anemometry tower (Unit: m/s)

| Height / m | 70 | 50 | 30 | 10 |
|---|---|---|---|---|
| 10 | 6.8 | 6.3 | 5.7 | 4.6 |
| 30 | 6.9 | 6.3 | 5.7 | 4.6 |
| 50 | 6.6 | 6.1 | 5.5 | 4.4 |
| 70 | 6.5 | 6.0 | 5.4 | 4.3 |
| Maniao measurements | 6.5 | 6.1 | 5.8 | 4.6 |

## 6 COMPARISON BETWEEN SIMULATED VALUE AND MEASURED VALUE THROUGH THE COMBINATION OF WEST AND WASP

The two simulated data sets which were the nearest to the eight anemometric towers were collected separately from WEST mesoscale grid points at a height of 70 m. They were keyed in to WAsP to calculate the average wind speed at the same height as that in the anemometric towers. Next, the average wind speed was compared with the measured values in the anemometric towers. Table 3 shows the comparison between the simulated and measured values of annual average wind speed at the height of 70 m.

Table 3 shows that the absolute error between simulated value and measured value is 0.2–0.6 m/s, while the relative error is 3%–9%. Thus, the effect of numerical simulation of wind energy resource by WEST and WEST+WAsP is equivalent in the coastal areas of Hainan province. However, the WEST+WAsP scheme can be used as a guide on acquiring the distribution of wind energy resource with resolution of 100 m and providing scientific basis for micro-location selection of wind fields.

Table 3. Comparison between simulated value and measured value through the combination of WEST and WAsP for the height of 70 m

| Tower name | Simulated value/ (m/s) | Measured value / (m/s) | Relative error / % |
|---|---|---|---|
| Yinggehai | 5.4 | 5.1 | 6 |
| Gancheng | 7.3 | 6.8 | 7 |
| Sigeng | 7.1 | 6.7 | 6 |
| haitou | 6.2 | 5.7 | 9 |
| E'man | 6.8 | 6.6 | 3 |
| Maniao | 6.3 | 6.5 | 3 |
| Yubao | 6.0 | 6.4 | 6 |
| Mutoulan | 6.8 | 7.2 | 6 |

## 7 CONCLUSIONS

After conducting the numerical simulation of wind energy resource in Hainan province and the areas along the seaside based on theoretical analysis by WEST, a numerical simulation system of wind energy resource, and testing the effect of the simulation of the data collected from meteorological stations and anemometric towers, the following conclusions can be reached.

(1) The classification of large-scale weather background field based on the geostrophic condition by WEST is theoretically sound; however, it lacks the description of local thermal effect. Under the condition that the local terrain is complicated and is affected significantly by thermal effect, this classification will easily be distorted and the simulated values will show large deviation as a result. Therefore, taking the influence of thermal effect into account during the classification of weather background field with the WEST model is more reasonable and objective.

(2) The result of the WEST simulation of the average distribution of wind energy resource for the 30 years agrees with the result of a general survey of wind energy in Hainan province. When compared with the measured values taken from the stations, however, because of changes in the environment around the stations, the simulated values are larger than the measured ones.

(3) The comparison of WEST-simulated values of average wind speed with the measured values from anemometric towers show that the higher the point, the smaller the relative errors of the simulated value. At the height of 70 m, the relative error between the simulated and measured values of annual average wind speed is less than 9%.

(4) Compared to the measured value of annual average wind speed at the height of 70 m, the relative

error of the simulated value determined with the combined model of WEST and WAsP is less than 9%. This means that conducting numerical simulation of wind energy in the coastal and offshore areas of Hainan province using the combined model of WEST and WAsP is feasible.

Certainly, there are some limitations and problems in WEST model and further improvement and modification are needed. Nonetheless, WEST is a generally good simulation model of wind energy resource with high resolution. It simulates the wind condition well in flat terrain and can be applied to assess the wind energy resource in the coastal areas. Moreover, the result of the simulation can be used as input field (of climate) in WAsP to simulate the micro-scale wind condition and provide scientific basis for micro-location selection of wind fields.

## REFERENCES:

[1] JOHN L W, REBECCA J B, WILLIAM R B. The statistical prediction of offshore winds from land-based data for wind-energy applications [J]. Boundary-Layer Meteor., 2001, 101(3): 409-433.
[2] LANGE B, LARSEN S E, HOJSTRUP J. The wind speed profile at offshore wind farm sites [C]// Preprint, Dewek 2002, Wilhelmshaven: 1-4.
[3] YUAN Chun-hong, XUE Heng, YANG Zhen-bin. A numerical modeling study for offshore wind speed [J]. J. Solar Energy. 2004, 25(6): 740-743.
[4] JIANG Dong, WANG Jian-hua. Wind energy resources assessment in the coastal zones based on spatial information techniques [J]. Prog. Geography, 2004, 23(6): 41-48.
[5] YU W, BENOIT R, GIRARD C, et al. Wind Energy Simulation Toolkit (WEST): a wind mapping system for use by the wind-energy industry [J]. Wind Eng., 2006, 30: 15-33.
[6] GIRARD C, BENOIT R, DESGAGNÉ M. Finescale topography and the MC2 dynamics Kernel [J]. Mon. Wea. Rev., 2005, 133(6): 1 463-1 477.
[7] TANGUAY M, ROBERT A, LAPRISE R. A semi-implicit semi-Lagrangian fully compressible regional forecast model [J]. Mon. Wea. Rev., 1990, 118: 1 970-1 980.
[8] THOMAS S, GIRARD C, BENOIT R, et al. A new adiabatic kernel for the MC2 model [J]. Atmos-Ocean. 1998, 36(1): 241-270.
[9] TROEN I, PETERSEN E L. The Wind Atlas model (Chapter 8) [M]. European Wind Atlas, Denmark: Risø National Laboratory, 1989: 565-593.
[10] KALNAY E, KANAMITSU M, KISTLER R, et al. The NCEP/NCAR 40-year reanalysis project [J]. Bull. Amer. Meteor. Soc., 1996, 77(3): 437-471.
[11] ZUO Hong-chao, LU Shi-hua, HU Yin-qiao. Variation trend of yearly mean air temperature and precipitation in China in the last 50 years [J]. Plateau Meteor., 2004, 23(2): 238-244.
[12] ZHANG Y, SPERBER K R, BOYLE J S. Climatology and interannual variation of the East Asian winter monsoon: results from the 1979-95 NCEP/NCAR reanalysis [J]. Mon. Wea. Rev., 1997, 125(10): 2 605-2 619.
[13] ZHANG Qiong, QIAN Yong-fu. Monthly mean surface albedo estimated from NCEP/NCAR reanalysis radiation data [J]. Acta Geographica Sinica, 1999, 54(4): 309-317.
[14] WANG Shu-yu. The studies of East Asia regional climate modeling and soil moisture initialization [D]. Beijing: Institute of Atmospheric Physics, Chinese Academy of Sciences. 2003.
[15] TANG Jian-ping, SU Bing-kai, ZHAO Ming, et al. Long term climate change numerical simulation in east Asia [J]. Acta Meteor. Sinica, 2004, 62(6): 752-763.

**Citation:** XING Xu-huang, ZHU Rong, ZHAI Pan-mao et al. High-resolution numerical simulation of wind energy resource in Hainan province and its offshore waters. *J. Trop. Meteor.*, 2010, 16(3): 292-298.